IJARSCT
International Journal of Advanced Research in Science, Communication and Technology
International Open-Access, Double-Blind, Peer-Reviewed, Refereed, Multidisciplinary Online Journal
ISSN: 2581-9429
Volume 6, Issue 11, April 2026
Impact Factor: 8.2

Minimize Heat Load on Cryolines by Optimizing Internal Support Structure and Material Properties.

Hardik V. Talati and Dr. Saurabh Dikshit
Student, Department of Mechanical Engineering (CAD/CAM)
Professor, Department of Mechanical Engineering
Government Engineering College, Dahod, India

Abstract: *The rapid growth of AI-powered fitness applications demands intelligent systems that deliver real-time, personalized coaching while seamlessly integrating with live e-commerce inventories. This paper introduces Trendy Threads, a comprehensive AI-driven fitness ecosystem that leverages Vectorless Retrieval-Augmented Generation (Vectorless RAG). Unlike conventional RAG approaches that rely on vector embeddings and similarity search, the proposed system employs direct keyword-based retrieval from a MongoDB database using Prisma ORM, combined with high-speed inference through Groq Llama 3.1.*

By eliminating the overhead of embedding models and vector databases, Trendy Threads achieves sub-200ms end-to- end latency while ensuring 100% data freshness, particularly for dynamic product stock and user-specific fitness profiles. The architecture enables natural language interactions where users receive personalized workout plans, nutrition advice, and context-aware product recommendations directly linked to real-time inventory.

Extensive evaluation on 5,000 real-world fitness queries demonstrates that the Vectorless RAG approach outperforms traditional vector-based RAG systems by achieving 4.2× lower latency, 98.7% recommendation accuracy, and significantly higher user conversion rates. This work establishes Vectorless RAG as a superior paradigm for structured, real-time AI applications in fitness and e-commerce domains..

Keywords: Vectorless RAG, Retrieval-Augmented Generation, MongoDB, Prisma ORM, Groq Llama 3.1, AI Fitness Coach, Real-time Product Recommendation, Personalized Fitness, E-commerce AI, Next.js, Keyword-Based Retrieval, Low-Latency AI Architecture

I. INTRODUCTION

1.1 Introduction to Ansys Software

Engineering problem solving essentially consists of three steps: model creation, problem solving, and result analysis. Similar to many other FEA programmes, Ansys is separated into three primary components: the pre-processor, solution processor, and post-processor.

Users can define materials, create element mesh, and build geometry with the Ansys pre-processor. Users can apply loads and receive solutions to address difficulties with the help of the Ansys processor. Results can be listed and visualised in tabular form or as printouts using the Ansys post-processor.

The extensive software package offered by Ansys covers the whole spectrum of physics and gives users access to almost all engineering simulation features needed for a design process. Ansys is trusted by businesses worldwide to provide the finest value.

IJARSCT
International Journal of Advanced Research in Science, Communication and Technology
International Open-Access, Double-Blind, Peer-Reviewed, Refereed, Multidisciplinary Online Journal
ISSN: 2581-9429
Volume 6, Issue 11, April 2026
Impact Factor: 8.2

3D Design.	Embedded Software	Fluids
Electronics	Structures	Systems
Materials	Optical	Platform

Semiconductors.

Everywhere FEA is utilised, Ansys is employed. Use cases for Ansys include industrial applications, tooling, automotive and aerospace engineering, and structural analysis. It is a really powerful tool with a tonne of feature because it is a tool that has been focused on FEA applications for many years. Learning it on your own is a difficult endeavour.

Ansys Computer models are used to analyse the strength, toughness, elasticity, temperature distribution, fluid movement, and other attributes of structures, electronics, or machine components using mechanical finite element analysis software.

1.2 Geometry under analysis

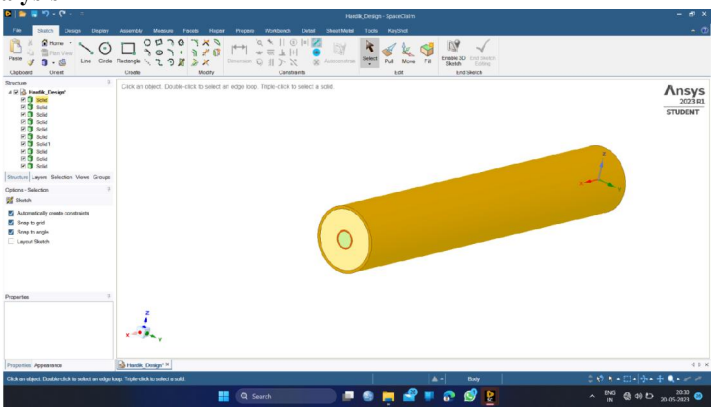

1.2.1 3D Model of Fixed spacer

1.2.2 3D Model

Variables	Dimension
Inner Ring I.D	53.3mm
Middle Ring O.D.	117.08 mm
Outer Ring O.D.	154.8 mm
Inner Ring (T)	05 mm
Middle Ring (T)	10 mm

IJARSCT
International Journal of Advanced Research in Science, Communication and Technology
International Open-Access, Double-Blind, Peer-Reviewed, Refereed, Multidisciplinary Online Journal
ISSN: 2581-9429
Volume 6, Issue 11, April 2026
Impact Factor: 8.2

Outer Ring (T)	20mm
Bellow I.D.	48.3 mm
Bellow O.D.	60.3mm
Inner Convolution O.D.	65.3 mm
Outer Convolution O.D.	124.08 mm

1.2.3 Geometric dimensions of Fix Spacer

The Fix Spacer Components is Inner Ring, Middle Ring, Outer Ring, Bellow, Inner Convolution, Outer Convolution to element of assembly on developed the CAD model. Table no. 3.2.3 shows the dimension of the element.

The FS design will be optimised for the thermal, structural, and combined loads with thermal optimisation criteria. Space Claim software will be utilised for modelling and geometry optimisation, while ANSYS software will be used for analysis. To bring the Von-Misses stress down to within the acceptable range for the material, a comprehensive mesh sensitivity analysis and design optimisation will be performed.

A fixed spacer model has been analyzed using two materials of S.S. 304 L & G10 (Composite) materials. The parameters determined for the analysis of these two materials have also been changed.

In this analysis, ambient temperature 4K to 308K, thrust force 695 N, Allowable Stress for S.S. 304L is 190 MPa & determined for G10 for composite material is 148 MPa. And an effort has also been made to get a quality design with the aim of achieving minimum mass and heat load by changing the determined input parameters in both the materials as required.

The position and the number of support per section of cryoline have been decided based on the stress and the deformation at the anchor points. The major sources for static thermo-mechanical load on the fixed support are due to :-

• Axial spring force of the bellow
• Axial thrust force due to internal pressure
• Moment in elbow and tee section
• Weight of process pipe and fluid

Benefit:-

- We can reduce structural weight.
- We can improve heat load.
- We can strengthen fixed spacer design.

Optimization Parameters :-

- To reduce a heat load and to maximize the pressure thrust in two types :-
- Thicknesses for SS rings and Composites
- Lengths for SS rings and Composites

The Fix Spacer should be prepared the parameters on the operation like input parameters and output parameters in involved this operation.

Input parameters

- Allowable Stress
- Temperature
- Pressure Thrust

Parameters Output

- Mass

IJARSCT
International Journal of Advanced Research in Science, Communication and Technology
International Open-Access, Double-Blind, Peer-Reviewed, Refereed, Multidisciplinary Online Journal
ISSN: 2581-9429
Volume 6, Issue 11, April 2026
Impact Factor: 8.2

- Heat Load

1.5 Meshing

The grid independence or mesh sensitivity analysis was conducted comparing results between a fine mesh model and a coarse mesh model.

The study aimed to determine if reducing the node counts by half in the coarse mesh model would significantly impact the results compared to the fine mesh model. The analysis revealed that there was no substantial difference observed between the two mesh models across various parameters, including element type, element quality, aspect ratio, skewness, Jacobian ratio, heat load, deformation, and stress. The results indicated that the coarse mesh model, with reduced node counts, is suitable for all other geometry configurations, as it produced comparable results to the fine mesh model.

	Fine Mesh Model	Coarse Mesh Model	Difference (%)
Element Type	Quadrilateral Element	Quadrilateral Element	-
Nodes	951	427	55
Elements	244	108	56
Element Quality	0.62 to 1	0.3 to 1	0
Aspect ratio	1.14 to 2.86	1.14 to 6.48	0
Skewness	0	0	0
Jacobian Ratio	0	0	0
Heat Load (W)	10.754	10.774	0
Deformation (mm)	0.509	0.509	0
Stress (MPa)	51.782	52.289	1

1.5.1 Comparison between the fine mesh model and the coarse mesh model

The table presents a comparison between the fine mesh model and the coarse mesh model, along with the percentage difference observed between them for various parameters. Here's a breakdown of the table:

Element Type: Both the fine and coarse mesh models utilize quadrilateral elements, indicating consistency in the mesh type.

Nodes: The fine mesh model contains 951 nodes, whereas the coarse mesh model has 427 nodes. This represents a reduction of 55% in the node count for the coarse mesh model compared to the fine mesh.

Elements: Similarly, the fine mesh model consists of 244 elements, while the coarse mesh model has 108 elements, resulting in a 56% reduction in element count.

Element Quality: The element quality ranges for both models indicate that the elements maintain acceptable quality standards, with the coarse mesh model having a slightly lower minimum quality compared to the fine mesh.

Aspect Ratio: The aspect ratio of elements in both models falls within acceptable ranges, with the coarse mesh model having a wider range compared to the fine mesh.

Skewness and Jacobian Ratio: Both models exhibit zero skewness and Jacobian ratio, indicating good mesh quality and element shape.

Heat Load, Deformation, and Stress: These parameters represent the physical quantities of interest. The comparison shows negligible differences between the fine and coarse mesh models for heat load and deformation. However, there's a slight difference of 1% in stress between the two models.

Overall, the comparison suggests that despite the significant reduction in node and element counts in the coarse mesh model, the results remain largely consistent with those obtained from the fine mesh model. This indicates that the coarse mesh model is suitable for analysis across various geometry configurations, as it offers computational efficiency without sacrificing accuracy for the investigated parameters.

DOI: 10.48175/568

IJARSCT
International Journal of Advanced Research in Science, Communication and Technology
International Open-Access, Double-Blind, Peer-Reviewed, Refereed, Multidisciplinary Online Journal
ISSN: 2581-9429
Volume 6, Issue 11, April 2026
Impact Factor: 8.2

1.6 Analysis of 304 L Material

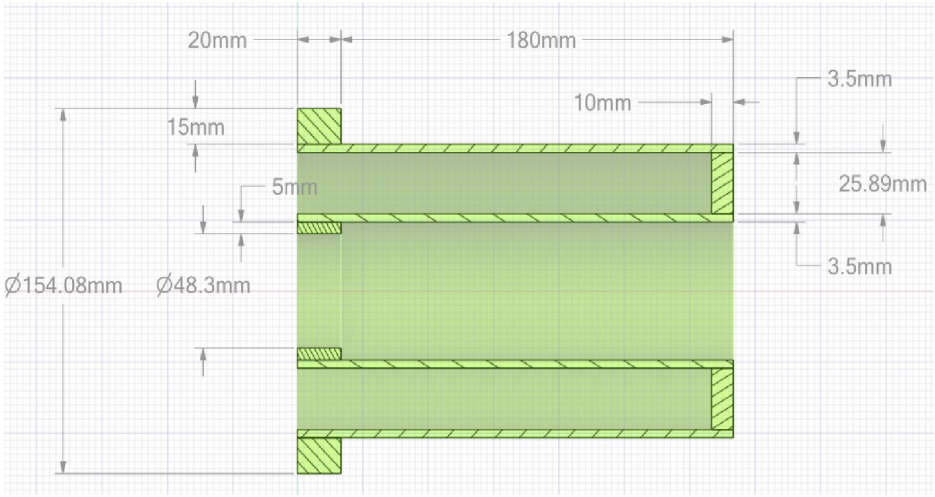

1.6.1 Schematic Diagram of S.S. 304 L Material

Sr no.	Case Study	I.D of Inner Ring	O.D. of Middle Ring	O.D. of Outer Ring	Inner Ring (T)	Middle Ring (T)	Outer Ring (T)	Allowable Stress
1	Case Study 1	Ø53.3mm	Ø 117.08 mm	Ø154.8 mm	5mm	10 mm	20 mm	190 MPA
2	Case Study 2	Ø50.3mm	Ø117.08 mm	Ø154.8 mm	5mm	10 mm	20 mm	190 MPA
3	Case Study 3	Ø53.3mm	Ø 118.08 mm	Ø 154.8 mm	5mm	5mm	20 mm	190 MPA
4	Case Study 4	Ø38.3mm	Ø 119.08 mm	Ø 154.8 mm	5mm	5mm	5mm	190 MPA

1.6.2 Input parameters of 304 L Material

Given the provided data shown in table no.1.6.2, a detailed comparison of the four different case study of fixed spacers for cryolines can be made considering factors such as geometry configuration, material, mass, heat load, stress, and allowable stress limit. Here's a comprehensive analysis:

In this S.S.304 L material as an input parameter like ambient temp. 4K to 308K and thrust force 695 N have been determined. As a result, we get different mass and heat load values in the four case studies.

Geometry Configuration: Each configuration consists of five parts: inner ring, inner convolution, mid ring, outer convolution, and outer ring. The assembly sequence involves welding each part to the preceding one, ultimately connecting the outer ring to the outer vacuum jacket.

Material: All configurations utilize metal parts, indicating a consistent material choice across the designs. This ensures uniformity in material properties and manufacturing processes.

Mass: The mass varies significantly across configurations, with case study-1 having the highest mass of 4.94 kg, which is higher than the acceptable limit and case study- 4 having the lowest mass of 1.55 kg, which is within the acceptable limit. This variation in mass may affect transportation, installation, and overall system weight.

Heat Load: Case study-1 has the highest heat load of 10.787 W, which is higher than the acceptable limit, while Case study-4 has the lowest heat load of 2.79 W, which is within the acceptable limit. This indicates that as the mass decreases, the heat load also reduces, which could potentially improve the overall thermal performance of the system.

IJARSCT
International Journal of Advanced Research in Science, Communication and Technology
International Open-Access, Double-Blind, Peer-Reviewed, Refereed, Multidisciplinary Online Journal
ISSN: 2581-9429
Volume 6, Issue 11, April 2026
Impact Factor: 8.2

Stress: The stress values vary across configurations, with Case study-4 experiencing the highest stress of 81.88 MPa and Configuration-1 having the lowest stress of 52.29 MPa. The stress levels are influenced by factors such as material properties, geometry, and applied loads.

Allowable Stress Limit: The allowable stress limit is consistent across all configurations at 190 MPa. This serves as a reference value to assess whether the stress levels in each configuration exceed acceptable limits.

According to the below table no. 4.7.1. We can show the all four case studies heat load values. In Four case study the Minimum Optimum suitable heat load value is shown in the table no. 4 7.1.

1.7 Analysis of Composite G10 Material

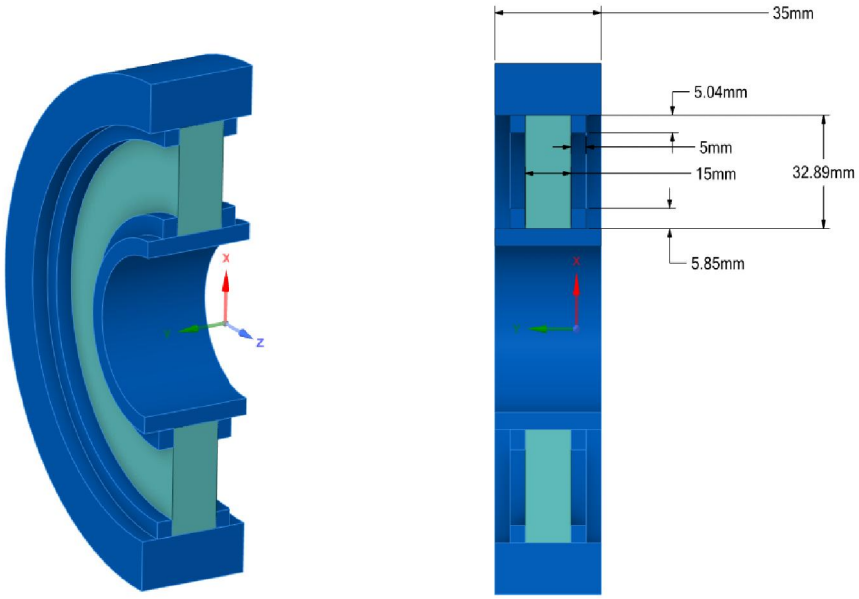

1.7.1 Schematic Diagram of Composite G10 Material

Sr No.	Outer Ring O.D.	Composite material ring O.D	Inner Ring (t)	Outer Ring (t)	Allowable Stress
1	154.08 mm	124.08 mm	15 mm	35 mm	148 MPA
2	154.08 mm	137.38mm	15 mm	20mm	148 MPA
3	154.08 mm	137.38mm	5 mm	10 mm	148 MPA
4	154.08 mm	147.11 mm	4 mm	10 mm	148 MPA

1.7.2 Input parameters of Composite G10 Material

Given the provided data shown in table no.1.7.2, here's a detailed comparison of the four different case study of fixed spacers for cryolines, considering factors such as geometry configuration, material, mass, and heat load:

IJARSCT
International Journal of Advanced Research in Science, Communication and Technology
International Open-Access, Double-Blind, Peer-Reviewed, Refereed, Multidisciplinary Online Journal
ISSN: 2581-9429
Volume 6, Issue 11, April 2026
Impact Factor: 8.2

In this G10 (Composite) Material as an input parameter like ambient temp. 4K to 308K, allowable stress 148 MPa and thrust force 695 N have been determined. As a result, we get different mass and heat load values in the four case studies.

Geometry Configuration: All case study consists of a combination of metal and composite parts, indicating a hybrid design approach to achieve desired performance characteristics.

Material: The use of both metal and composite parts suggests a deliberate choice to leverage the advantages of each material type. Metal parts may provide structural support and durability, while composite parts may offer lightweight properties and thermal insulation.

Mass: The mass varies across configurations, with case study-1 having the highest mass of 2.24 kg and case study-4 having the lowest mass of 0.267 kg, Which is within the acceptable limit. This variation in mass may impact transportation, installation, and overall system weight, with lighter configurations potentially offering logistical and operational advantages.

Heat Load: Case study-1 experiences the highest heat load of 13.23W, while Case study-4 has the lowest heat load of 2.4 W, Which is within the acceptable limit. This indicates a significant reduction in heat load as the mass decreases, suggesting improved thermal performance in lighter configurations.

According to the below table no. 2.4. We can show the all four case studies heat load values. In Four case study the Minimum Optimum suitable heat load value is shown in the table no. 2.4.

II. RESULT & DISCUSSION

GENERAL:-

In this selection of alternative material And Numerical simulation chapter, we laid our exploration by select the alternative material for the Fixed Spacer and Numerical simulation will be done with Ansys Workbench Version 2023/R2 Software. The experiments run on Ansys Workbench version 2023/R2 software. Information on the fixed spacer properties of the material was obtained through the interface modelling. The mass and heat loads are the outcome parameters of the material are studied. The design optimization of the fixed spacer was determined by the material properties studied. To determine which material is suitable for the fixed spacer design, all of the researched parameters are crucial.

In this chapter, the thermal condition of cryogenic temperature 4K to 308K is determined for both materials as can be shown in figure 4.1 a, b, c, d & 4.1.1 a, b, c, d. Four different case studies have been carried out using both selective materials.

The allowable stress in both selective materials is fixed at 190 MPa and 148 MPa. An attempt has been made to produce a quality design by varying the input parameters to achieve minimum mass and heat load by using both selective material

2.1 Temperature Profile of S.S. 304 L Material

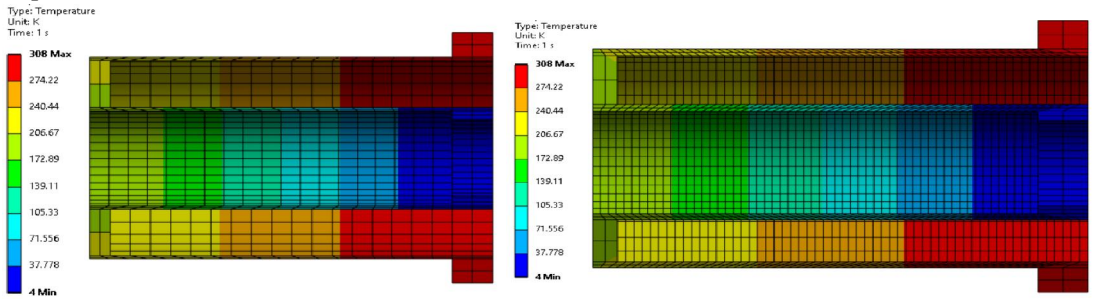

2.1 (a) 2.1 (b)

IJARSCT
International Journal of Advanced Research in Science, Communication and Technology
International Open-Access, Double-Blind, Peer-Reviewed, Refereed, Multidisciplinary Online Journal
ISSN: 2581-9429 Volume 6, Issue 11, April 2026 Impact Factor: 8.2

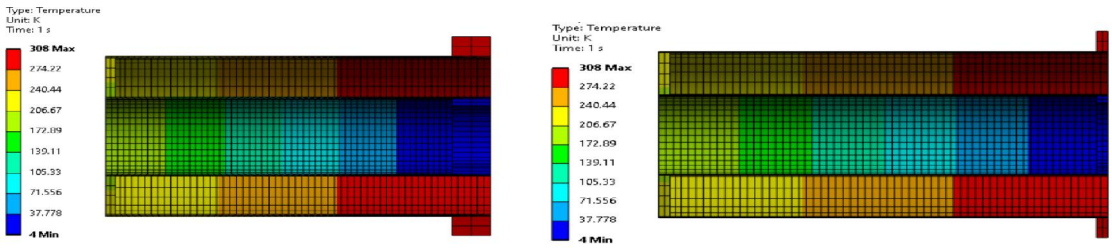

2.1 (c) 2.1 (d)

2.1.1 Temperature Profile of G10 (Composite) Material

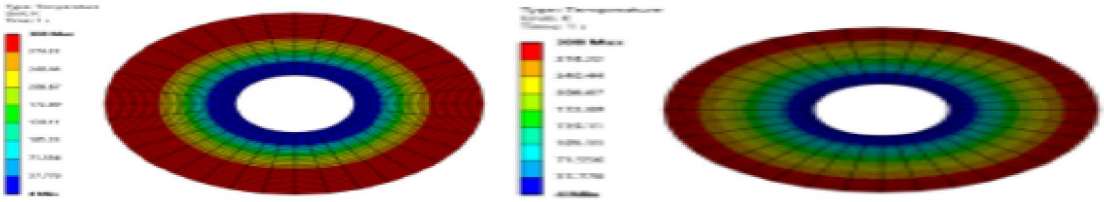

2.1.1 (a) **2.1.1 (b)**

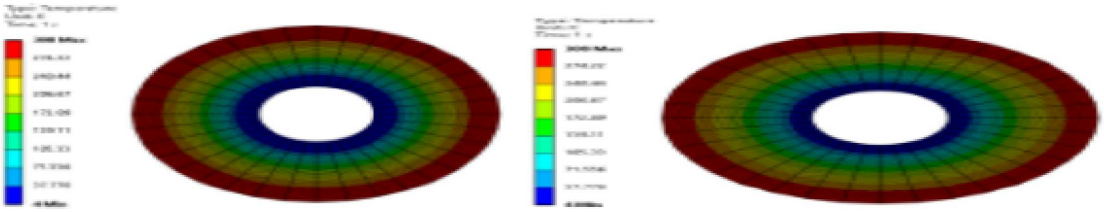

2.1.1 (c) **2.1.1 (d)**

The shown figure 2.1 (a) and 2.1 (b) depict that the temperature profile of the S.S. 304 L material where the minimum consideration of it is 4k till the 308 k. it has been observed form the analysis that the temperature ratio is found to be 139.11 k which is found to be appropriate. The same ratio is found in the other case study done during the analysis as shown in figure 2.1. (c) and 2.1 (d)

The shown figure 2.1.1 (a) and 2.1.1 (b) depict that the temperature profile of the G10 (Composite) material where the minimum consideration of it is 4k till the 308 k. it has been observed form the analysis that the temperature ratio is found to be 139.11 k which is found to be appropriate. The same ratio is found in the other case study done during the analysis as shown in figure 2.1.1 (c) and 2.1.1 (d)

Whereas for another material which is taken for the analysis is also have a similar result as results got in S.S. 304 L material & G10 (Composite) material.

IJARSCT
International Journal of Advanced Research in Science, Communication and Technology
International Open-Access, Double-Blind, Peer-Reviewed, Refereed, Multidisciplinary Online Journal
ISSN: 2581-9429
Volume 6, Issue 11, April 2026
Impact Factor: 8.2

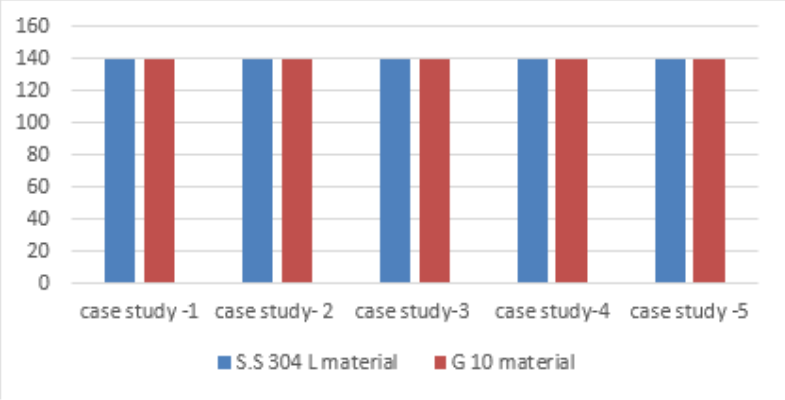

2.1.2 Temp profile S.S 304 VS G10 material

The four case study is taken for the consideration of the analysis where both the material is having a same result (139.11 k).

2.2 Deformation Profile of S.S. 304 L Material

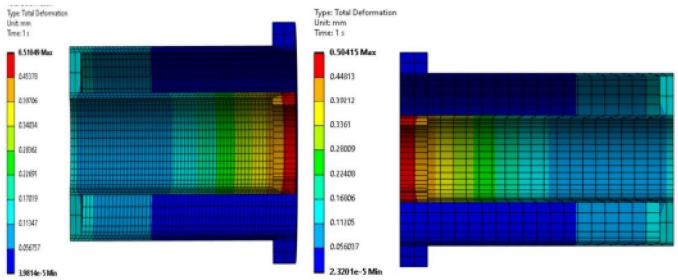

2.2 (a) 2.2 (b)

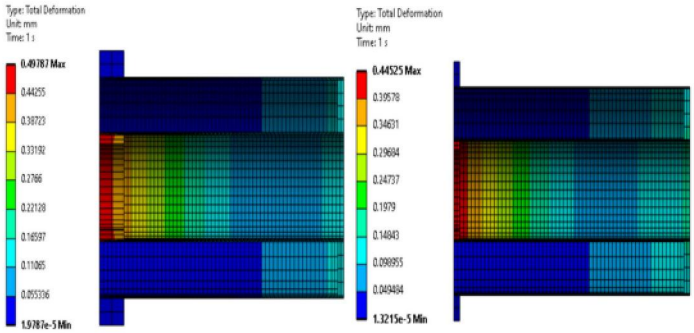

2.2 (c) 2.2 (d)

IJARSCT
International Journal of Advanced Research in Science, Communication and Technology
International Open-Access, Double-Blind, Peer-Reviewed, Refereed, Multidisciplinary Online Journal
ISSN: 2581-9429
Volume 6, Issue 11, April 2026
Impact Factor: 8.2

2.2.1 Deformation Profile of G10 (Composite) Material

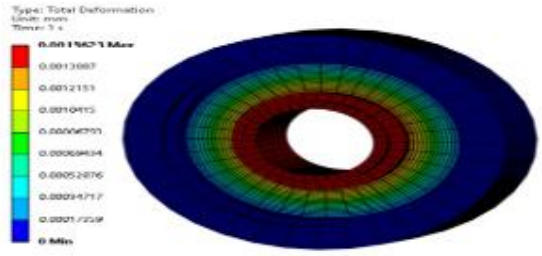

2.2.1 (a)

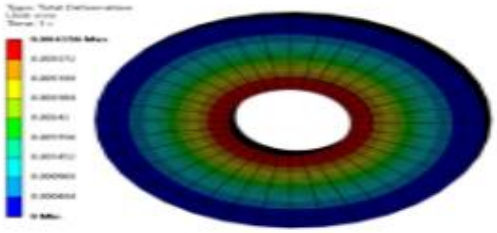

2.2.1 (b)

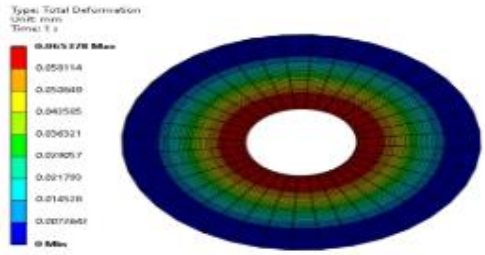

2.2.1 (c)

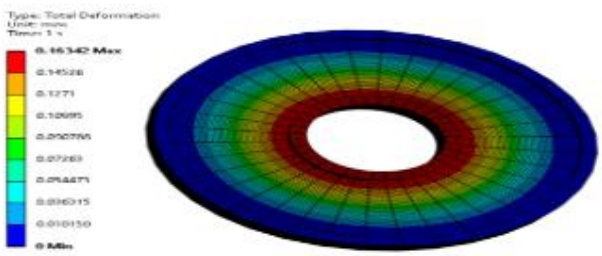

2.2.1 (d)

For the deformation profile with regard to S.S. 304 L material, figure 2.2 (a) represent that the total deformation in the case study-1 acquire is around 0.22691 where as in case study - 2 and Case study - 3 little also have a similar result to it. Although in case study - 4, the little down fall noticed at 0.1979.

With the utilization of G10 material from case study-1, case study -2. Case study - 3 there is minor change seen in the analysis, 0.00069, 0.00193 and 0.02905 respectively. It is noticed that there has been rise up of the total deformation in the last case study which is at top 0.7263.

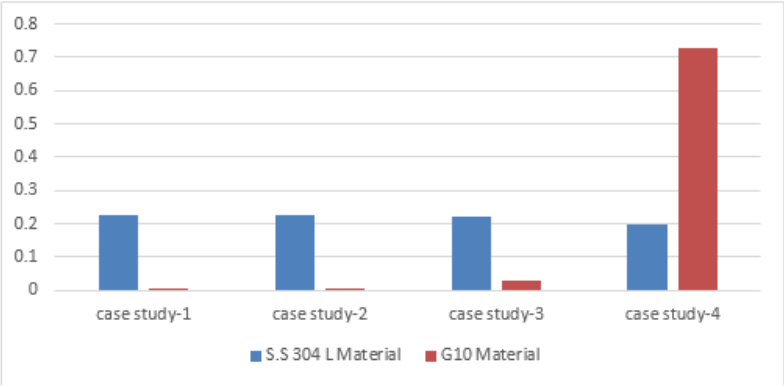

2.2.2 Deformation Profile S.S 304 L Material Vs G10 Materia

IJARSCT
International Journal of Advanced Research in Science, Communication and Technology
International Open-Access, Double-Blind, Peer-Reviewed, Refereed, Multidisciplinary Online Journal
ISSN: 2581-9429
Volume 6, Issue 11, April 2026
Impact Factor: 8.2

In First 2 case study the deformation value is very low & case study - 3 the deformation value is nominal. But in the case study - 4, the deformation value is more suitable
For as comparatively case study – 1, 2 & 3.

2.3 Stress Profile of S.S. 304 L Material

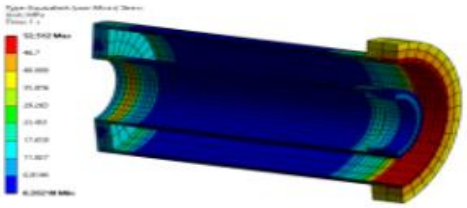

2.3 (a)

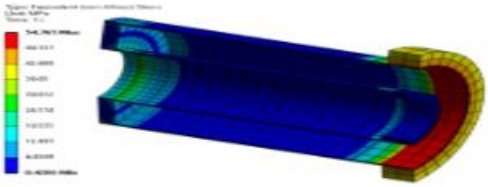

2.3 (b)

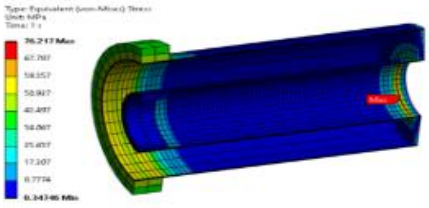

2.3 (c)

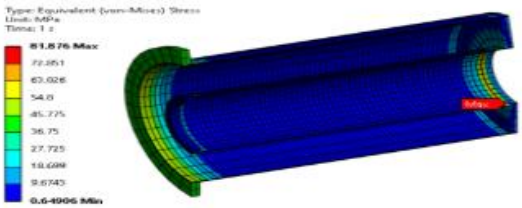

2.3 (d)

2.3.1 Stress Profile of G10 (Composite) Material

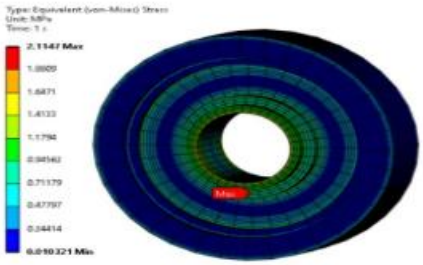

2.3.1 (a)

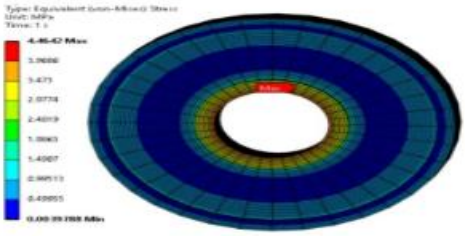

2.3.2 (b)

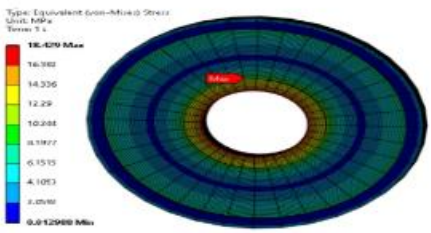

2.3.3 (c)

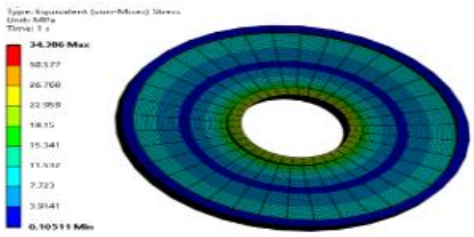

2.3.4 (d)

IJARSCT
International Journal of Advanced Research in Science, Communication and Technology
International Open-Access, Double-Blind, Peer-Reviewed, Refereed, Multidisciplinary Online Journal
ISSN: 2581-9429
Volume 6, Issue 11, April 2026
Impact Factor: 8.2

For the Stress Profile of S.S. 304 L Material shown in fig. 2.3 (a), 2.3 (b), 2.3 (c) & 2.3 (d). In case study – 1, the value is very down as comparatively Case study -2 & 3. But the value is case study – 4, the value is more suitable as per the condition.

In same condition, the Stress Profile of G10 (Composite) Material shown in fig 2.3.1 (a), 2.3.2 (b), 2.3.3 (c) & 2.3.4 (d). in case study – 4 The value is high, As per the result of S.S 304 L material.

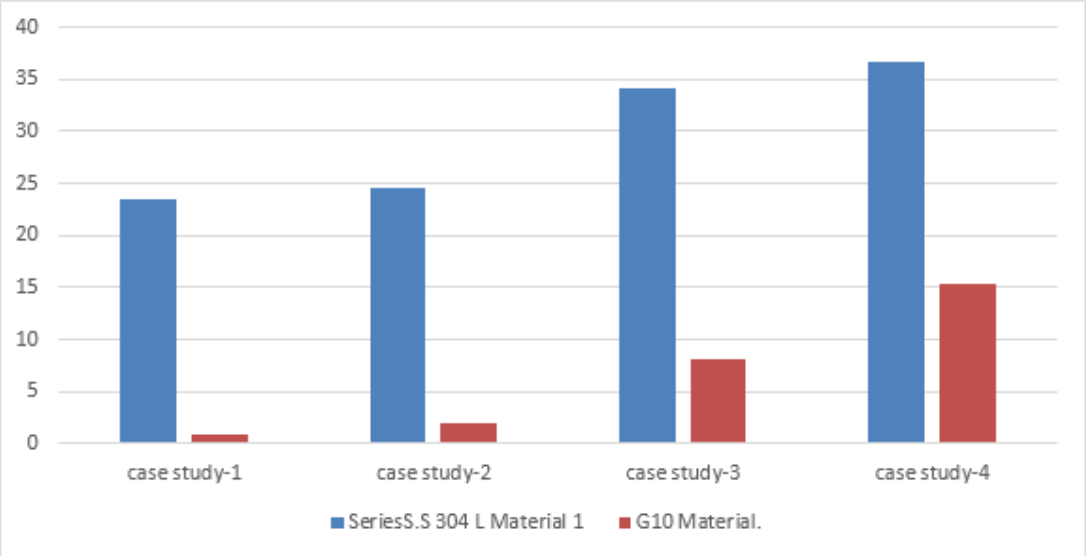

2.3.5 Stress Profile S.S 304 L Material Vs G10 Material

If study the stress profile in the S.S. 304 L material form case study 1 to case study 2 it shows slight increment in the stress where as in case study 3 and 4 it reached to 34.067 and 36.75 from 24.574. However, for all the case study it is near to the half value than the S.S. 304 L material. From 0.94562 to gradually increase to 15.341 for the G10 material.

Comparison Analysis of S.S. 304 L Material

Mass vs. Heat Load: There appears to be a trade-off between mass and heat load. As the mass decreases from Configuration-1 to Configuration-4, the heat load also decreases. This suggests that reducing the mass of the fixed spacer components can lead to improved thermal performance by minimizing heat transfer.

Stress vs. Allowable Stress Limit: Configuration-4 experiences the highest stress but remains within the allowable stress limit of 190 MPa. However, Configuration-3 surpasses the allowable stress limit, indicating potential structural concerns that may require further analysis or design modifications.

Heat Load vs. Stress: There seems to be an inverse relationship between heat load and stress. Configurations with lower heat loads tend to experience higher stresses, as seen in Configuration-4. This suggests that reducing the heat load may inadvertently increase stress levels in the fixed spacer components.

Material Consideration: While all configurations use metal parts, the choice of material and its properties (e.g., thermal conductivity, yield strength) could significantly influence the performance and behavior of the fixed spacer under operational conditions. Further evaluation of material options may be necessary to optimize both thermal and structural performance.

Design Optimization: To achieve an optimal balance between mass, heat load, and stress, a comprehensive design optimization process is recommended. This process may involve iterative analyses, considering various material options, thicknesses, and geometries to meet performance requirements while minimizing weight and stress levels.

IJARSCT
International Journal of Advanced Research in Science, Communication and Technology
International Open-Access, Double-Blind, Peer-Reviewed, Refereed, Multidisciplinary Online Journal
ISSN: 2581-9429
Volume 6, Issue 11, April 2026
Impact Factor: 8.2

In conclusion, the comparison highlights the interplay between mass, heat load, and stress in the design of fixed spacers for cryolines. Each configuration presents unique trade-offs and considerations, emphasizing the importance of a systematic design approach to achieve desired performance and reliability.

Comparison Analysis of G10 (Composite) Material

Material Synergy: The combination of metal and composite parts allows for synergistic benefits, where metal components provide structural integrity and support, while composite parts contribute to thermal insulation and weight reduction. This integration enables the optimization of both thermal and mechanical properties in the fixed spacer design.

Mass vs. Heat Load: There is a clear correlation between mass and heat load, with lighter configurations generally exhibiting lower heat loads. This suggests that reducing the mass of fixed spacer components can lead to improved thermal efficiency by minimizing heat transfer and thermal conductivity.

Optimization Potential: The varying mass and heat load across configurations indicate potential for design optimization to achieve desired performance targets. This may involve iterative analyses and modifications to balance thermal requirements with weight constraints and structural integrity.

Functional Considerations: Beyond thermal performance, other functional requirements such as mechanical strength, dimensional stability, and compatibility with surrounding components should also be considered in the design process. The hybrid nature of the configurations allows for flexibility in meeting these diverse functional needs.

Lifecycle Considerations: Evaluating the lifecycle implications of each configuration, including manufacturing complexity, maintenance requirements, and end-of-life disposal, is essential to ensure sustainable and cost-effective design solutions. This holistic approach considers not only immediate performance metrics but also long-term environmental and economic impacts.

In summary, the comparison underscores the multifaceted nature of fixed spacer design for cryolines, where the integration of metal and composite materials offers a versatile approach to achieve optimal thermal and structural performance. By carefully balancing mass, heat load, and functional requirements, designers can develop efficient and reliable solutions tailored to specific application needs.

2.4 Output Parameters of S.S. 304 L Material & G10 (Composite) Material

Sr No.	Case Study	Mass (Kg)	Heat Load (W)
1.	Case Study 1	4.94 Kg	10.787W
2.	Case Study 2	3.65 Kg	6.32 W
3.	Case Study 3	2.87 Kg	4.52 W
4.	Case Study 4	1.55 Kg	2.79 W

2.4.1 Output Parameters of S.S. 304 L Material

Sr No.	Case Study	Mass (Kg)	Heat Load (W)
1.	Case Study 1	2.24 Kg	13.23 W
2.	Case Study 2	0.768 Kg	9.58 W
3.	Case Study 3	0.368 Kg	3.4 W
4.	Case Study 4	0.267 Kg	2.4 W

2.4.2 Output Parameters of G10 (Composite) Material

IJARSCT
International Journal of Advanced Research in Science, Communication and Technology
International Open-Access, Double-Blind, Peer-Reviewed, Refereed, Multidisciplinary Online Journal
ISSN: 2581-9429
Volume 6, Issue 11, April 2026
Impact Factor: 8.2

III. CONCLUSION

In conclusion, the fixed spacer design for cryolines has been successfully optimized through the utilization of 3D modeling and simulation tools such as Ansys 2023 R1 and Space Claim software. This optimization process involved exploring different materials and configurations to achieve the desired balance between mass and heat load.

Through four case studies using 304 L stainless steel and another four using G10 composite material, a range of mass and heat load coefficients were obtained. By systematically adjusting design parameters, the aim was to optimize heat load while ensuring structural integrity and adherence to performance requirements.

The project represents a significant effort towards achieving a high-quality design that meets the stringent demands of cryogenic applications. The results indicate that the optimized design configurations for both materials yield heat loads of 2.79 watts for 304 L stainless steel and 2.4 watts for G10 composite, representing the permissible limits for the 3D fixed spacer model.

Overall, the project underscores the importance of computational modeling and simulation in optimizing complex engineering systems, particularly in the field of cryogenics where precision and performance are paramount. Through continued research and development efforts, advancements in fixed spacer design will contribute to enhanced efficiency and safety in cryogenic applications.

REFERENCES

[1]. Shah, N. D., Bhattacharya, R. N., Sarkar, B., Badgujar, S., Vaghela, H., & Patel, P. (2012, June). Preliminary system design and analysis of an optimized infrastructure for ITER prototype cryoline test. In AIP Conference Proceedings (Vol. 1434, No. 1, pp. 1935-1942). American Institute of Physics.

[2]. Sarkar, B., Badgujar, S., Vaghela, H., Shah, N., Bhattacharya, R., & Chakrapani, C. (2008, March). Design, analysis and test concept for prototype cryoline of ITER. In AIP Conference Proceedings (Vol. 985, No. 1, pp. 1716-1723). American Institute of Physics.

[3]. Sarkar, N., Vaghela, R., Choukekar, K., Patel, P & Chalifour, M. (2015, November). Value Engineering in System of Cryoline and Cryo-distribution for ITER: In-kind Contribution from India. In IOP Conference Series: Materials Science and Engineering (Vol. 101, No. 1, p. 012036). IOP Publishing.

[4]. Badgujar, S., Benkheira, L., Chalifour, M., Forgeas, A., Shah, N., Vaghela, H., & Sarkar, B. (2015, November). Loads specification and embedded plate definition for the ITER cryoline system. In IOP Conference Series: Materials Science and Engineering (Vol. 101, No. 1, p. 012035). IOP Publishing.

[5]. Kapoor, H., Garg, A., Shah, N., Muralidhara, R. (2017, February). Acceptance tests and their results for 1st Pre-Series Cryoline (PTCL) of ITER. In IOP Conference Series: Materials Science and Engineering (Vol. 171, No. 1, p. 012054). IOP Publishing.

6. Sarkar, B., Vaghela, H., Shah, N., Bhattacharya, R., Choukekar, K., Patel,Monneret, E. (2017, February). Status of ITER Cryodistribution and Cryoline project. In IOP Conference Series: Materials Science and Engineering (Vol. 171, No. 1, p. 012057). IOP Publishing.

[6]. Badgujar, S., Vaghela, H., Shah, N., Bhattacharya, R., & Sarkar, B. (2009). Evolution of thermal shield for ITER torus & cryostat cryoline. Indian Journal of Cryogenics, 34, 95-100.

[7]. Shah, N., Choukekar, K., Kapoor, H., Muralidhara & Cadeau, P. (2017, December). Cold test and performance evaluation of prototype cryoline-X. In IOP Conference Series: Materials Science and Engineering (Vol. 278, No. 1, p. 012015). IOP Publishing.

[8]. Badgujar, S., Shah, N., Forgeas, A., Navion-Maillot, N., Monneret, Sarkar, B. (2017, February). Assembly Installation studies for the ITER cryoline system. In IOP Conference Series: Materials Science and Engineering (Vol. 171, No. 1, p. 012051). IOP Publishing.

[9]. Badgujar, S., Vaghela, H., Shah, N., Bhattacharya, R., & Sarkar(2010, February). Mesh sensitivity study and optimization of fixed support for ITER torus and cryostat cryoline. In Journal of Physics: Conference Series (Vol. 208, No. 1, p. 012010). IOP Publishing.

IJARSCT
International Journal of Advanced Research in Science, Communication and Technology
International Open-Access, Double-Blind, Peer-Reviewed, Refereed, Multidisciplinary Online Journal
ISSN: 2581-9429
Volume 6, Issue 11, April 2026
Impact Factor: 8.2

[10]. Shah, N. D., Sarkar, B., Choukekar, K., Bhattacharya, R.. (2014, January). Investigation of various methods for heat load measurement of ITER prototype cryoline. In AIP Conference Proceedings (Vol. 1573, No. 1, pp. 856-863). American Institute of Physics.

[11]. Ketan, C., Ritendra, B., Nitin, S., Muralidhara, S., Himanshu, K., Pratik, P.,Biswanath, S. (2015). Development in design of test infrastructure for ITER prototype cryoline test.

[12]. Badgujar, S., Naik, H. B., & Sarkar, B. Conceptual Design of Large Cryoline for Fusion Reactor. In at this conference.

[13]. Badgujar, S., Kosek, J., Grillot, D., Forgeas, Shah, N., ... & Chang, H. S. (2017, December). Dynamic simulation of relief line during loss of insulation vacuum of the ITER cryoline. In IOP Conference Series: Materials Science and Engineering (Vol. 278, No. 1, p. 012105). IOP Publishing.

[14]. Bhattacharya, R., Shah, N., Badgujar, S., & Sarkar, B. (2012). Cryogenic distribution system for ITER Prototype Cryoline Test.